EUROPHYSICS LETTERS

OFFPRINT

Vol. 71 • Number 5 • pp. 838–844

Elementary triangles in a 2D binary colloidal glass former

* * *

H. König

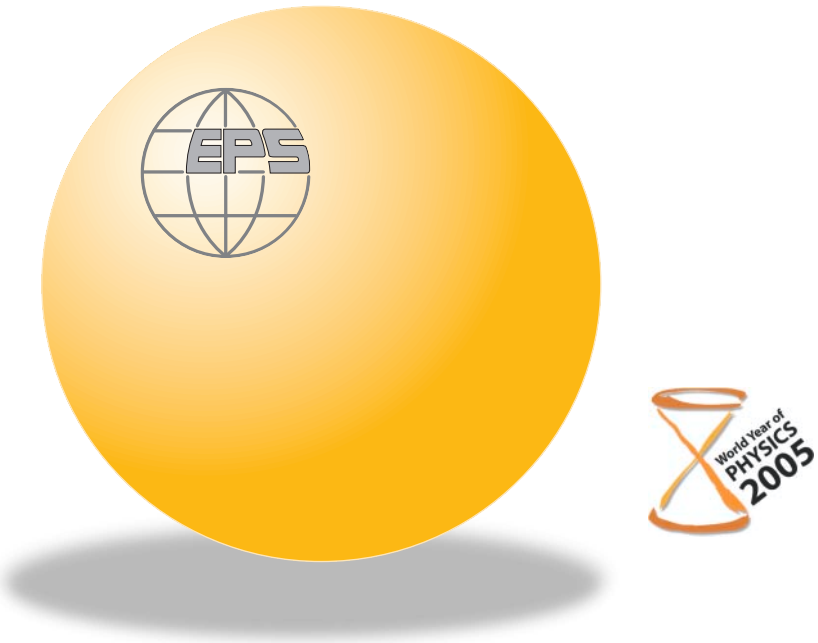

Published under the scientific responsability of the
EUROPEAN PHYSICAL SOCIETY
Incorporating
JOURNAL DE PHYSIQUE LETTRES • LETTERE AL NUOVO CIMENTO

EDP SCIENCES

EUROPHYSICS LETTERS

Europhysics Letter was launched more than fifteen years ago by the European Physical Society, the Société Française de Physique, the Società Italiana di Fisica and the Institute of Physics (UK) and owned now by 17 National Physical Societies/Institutes.

Europhysics Letters aims to publish short papers containing non-trivial new results, ideas, concepts, experimental methods, theoretical treatments, etc. which are of broad interest and importance to one or several sections of the physics community.

Europhysics letters provides a platform for scientists from all over the world to offer their results to an international readership.

EUROPHYSICS LETTERS 1 September 2005

Europhys. Lett., **71** (5), pp. 838–844 (2005)
DOI: 10.1209/epl/i2005-10153-8

Elementary triangles in a 2D binary colloidal glass former

H. KÖNIG
University of Konstanz, Department of Physics - 78457 Konstanz, Germany and Johannes-Gutenberg University of Mainz, Institute of Physics 55099 Mainz, Germany

received 29 March 2005; accepted in final form 4 July 2005
published online 3 August 2005

PACS. 82.70.Dd – Colloids.
PACS. 64.70.Pf – Glass transitions.
PACS. 61.20.Gy – Theory and models of liquid structure.

Abstract. – Particle positions of a two-dimensional (2D) binary colloidal glass former were measured video-microscopically. Local density-optimized structures of triangles of nearest-neighboring particles (TNNP) were found from the shortest pair-distances. These are referred to as elementary triangles (ET) —exactly one for each 3-particle combination of the two kinds of colloids. Clustering of ET-like TNNP implies larger distances between two particles, which generate the near-zone maxima in the pair-distribution functions. Tiling mismatches of different kinds of ET create structural frustrations. Increasing combination possibilities for the tiling of the different ET lead to the loss of long-range order for larger pair-distances. All features of the pair-distribution functions are qualitatively described.

Introduction. – Many materials exhibit a glass phase which can be described as solids with liquid-like structures and frozen-in particle dynamics. However, the physical properties of the various glass formers are mostly comparable in spite of different particle interactions [1, 2]. Thus, one might expect fundamental principles. If so, it would be satisfactory to explain different glass properties for only one single "model system" in order to understand these attributes for all the other glass formers as well. Using this reasoning, the amorphous microscopic near-zone structures of supercooled liquids are described by a novel method, investigating the experimentally measured particle coordinates of a special glass former, before postulating that these characteristic features can also be applicable to other glass formers.

In this paper, a two-dimensional (2D) binary colloidal glass former with repulsive particle interactions is studied. Analyzing the local amorphous structures, smallest particle arrangements in the monolayer were determined, which are triangles of nearest-neighboring particles (TNNP). For the two-component system there are four different 3-particle combinations. For each 3-particle combination, one local density-optimized triangle of idealized shape is found, which are subsumed as elementary triangles (ET). Tilings of these ET describe the complex short-range order in the amorphous 2D sample. Random tilings of different ET in the monolayer will not fill up the monolayer completely as structural frustrations occur. Thus, short-range peak positions, peak heights, frustration-related peak broadening, and the loss of long-range order in the partial radial pair-distribution functions can qualitatively be understood.

Experiment. – The setup is identical to that in [3] for monodisperse colloidal suspensions. More details about the binary mixture and why the investigated 2D system are glass formers are discussed in [4–6]. Here, we only briefly introduce the experiment.

In a two-component suspension of monodisperse superparamagnetic PMMA spheres, the big (b) colloids (Dynabeads M-450, uncoated [7]) have a diameter of $4.7\,\mu$m and a magnetic susceptibility $\chi_b = 6.2 \cdot 10^{-11}\,\mathrm{A\,m^2/T}$, while the small ($s$) colloids (dried Dynabeads M-280 uncoated [7]) have a diameter of $2.8\,\mu$m and a magnetic susceptibility $\chi_s = 6.6 \cdot 10^{-12}\,\mathrm{A\,m^2/T}$. The induced magnetic moments $M(B)$ of the colloids depend on the applied magnetic field B given by $M(B) = \chi(B) \cdot B$. For B-values up to 15 mT, $\chi_b(B)$ remains constant, while $\chi_s(B)$ decreases above 3 mT because of saturation effects, reaching about 65% of χ_s at 7 mT [4].

The colloids were confined to 2D due to gravity lying on a completely flat adjusted water-air interface of hanging droplet geometry. In the suspension, the thermally fluctuating big and small colloids interact with their induced magnetic moments, tuneable by a homogeneous external magnetic field B applied perpendicular to the water-air interface. The time-dependent particle coordinates were determined by video-microscopy in real time.

During an experiment the room temperature, T, the number area density, ρ, and the ratio, ξ, of the number N_s of small particles to the number $(N_b + N_s)$ of all colloids remain constant. Hence, only B controls the strength of the particle repulsion by the parallelly aligned induced magnetic moments. Other in-plane particle interaction potentials can be neglected [3]. The system is characterized by an interaction parameter, Γ, that is proportional to the magnetic energy E_m divided by $k_B T$. Thus, Γ corresponds to an inverse system temperature:

$$\Gamma = \pi^{3/2} \frac{E_m}{k_B T} = \frac{\mu_0}{4\pi} \frac{B^2 (\rho\pi)^{3/2}}{k_B T} \left(\xi \cdot \chi_s + (1-\xi) \cdot \chi_b\right)^2 . \tag{1}$$

This "model glass former" exhibits several advantages. The 2D confinement simplifies the observation of particle positions and the analysis of local structures. The restriction to two well-defined types of colloids reduces the number of microscopic particle arrangements. The repulsive potential leads to an energy landscape with a well for each particle. The highest dividend derives from the access to the time-dependent particle coordinates allowing us to investigate local particle configurations and short-time up to long-time relaxation processes for isotropic to strongly supercooled liquids [5]. Here, the amorphous structure in supercooled liquids is studied.

Local density-optimized structures. – In fig. 1a, the partial radial pair-distribution functions, $g_{ij}(r)$, of the different pairs ij of big (b) or small (s) colloids for the binary 2D colloidal suspension of fig. 2 are plotted. Additionally, a hard-disc approximation (HDA) of the big and small particles is introduced because of the sharp first maxima of $g_{ij}(r)$. The disc radii are determined from the half distance of the first maximum for the pairs bb and ss. These disc radii arise from the long-range repulsion of all magnetic moments in the 2D sample and are referred to as magnetic-field radii (MFR) in contrast to the hard-sphere radii of the particles themselves. In fig. 1a, the MFR ratio of big to small colloids is determined to be 2.15. Since systems of $\Gamma > 300$ have a well-defined cage-effect [4], *e.g.* a clear visible plateau in the mean-square displacements, the investigated sample of $\Gamma = 411$ remains in a strongly supercooled state.

The sum of the MFR of a big and a small colloid in the HDA is approximately 7% greater than the bs-pair-distance deduced from the first maximum of $g_{bs}(r)$, shown in fig. 1a. This fact is sufficient to use the HDA for the particle size in spite of the $1/r^3$-potential. Thus, in fig. 2, circles of the MFR are drawn around the big and small colloids, on top of the video image. For bs nearest-neighboring colloids, the MFR overlap. Also, discs often penetrate each other because of the softness of the $1/r^3$-potential and the thermal particle fluctuations.

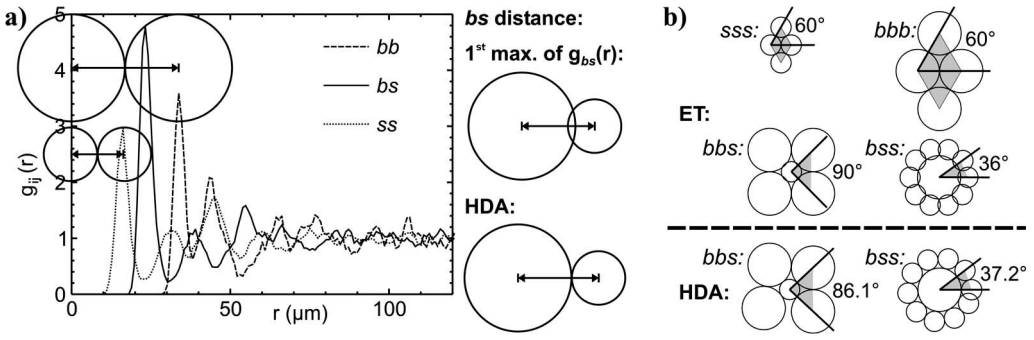

Fig. 1 – a) Partial radial pair-distribution functions $g_{ij}(r)$ of the binary 2D colloidal mixture shown in fig. 2. Therein, the magnetic-field radii (MFR) are clarified by the hard-disc approximation (HDA), *e.g.*, by the half distance of the first maximum for the pairs *bb* and *ss*. Notice that the real distance of the first maximum of $g_{bs}(r)$ is smaller than the *bs*-pair-distance obtained from the HDA. b) Isosceles elementary triangles (ET) for the four different 3-particle combinations of big and small particles can be obtained from the MFR while the particles slightly overlap for the *bbs* and *bss* ET. However, *bbs* and *bss* triangles of touching discs in the HDA do not allow local space filling.

For the four different 3-particle combinations of TNNP local density-optimized structures are observed, built up by identical isosceles triangles, for which all MFR of the colloids touch or slightly overlap. Those idealized local densely packed 3-particle combinations are defined as "elementary triangles" (ET). For the 3-particle combinations *sss* and *bbb* the ET are equilateral, *bbs* ET form right triangles, and *bss* ET have an angle of 36° at the big particle (compare the upper part of fig. 1b with fig. 2). Additionally, particle arrangements can consist of several ET of only one kind, namely "crystallite clusters" (CC), and assemblies of different CC without structural mismatch, termed as "multi crystallite clusters" (MCC). CC of *bbb* and

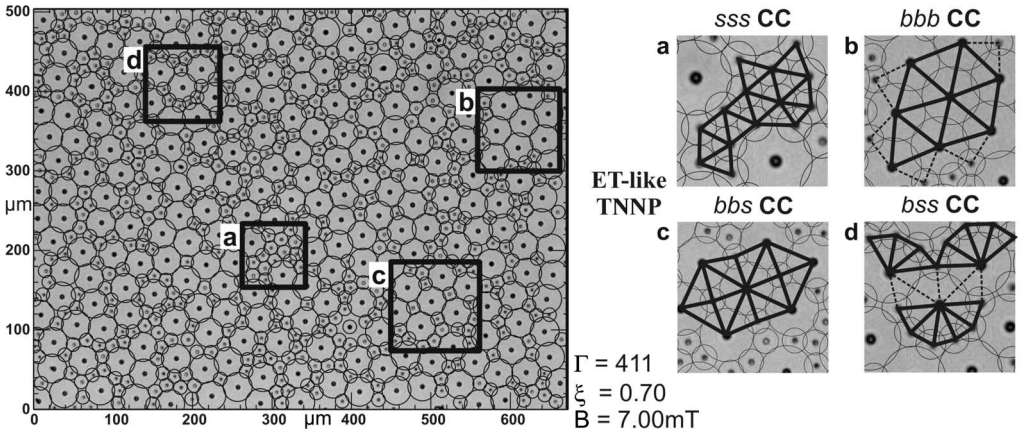

Fig. 2 – Video image with sketched magnetic-field radii by circles around the particles. In the supercooled sample, triangles of nearest-neighboring particles (TNNP) often form local-density-optimized shapes such as those of elementary triangles (ET), shown in the upper part of fig. 1b. Some crystallite clusters (CC) are marked by lines, added ET-like TNNP of other 3-particle combination by dashed lines, forming multi crystallite clusters with the central CC.

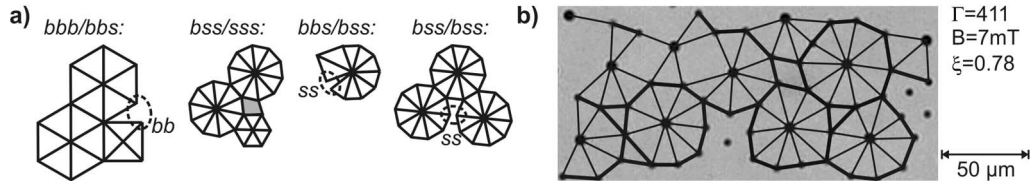

Fig. 3 – a) Some combinations of crystallite clusters or multi crystallite clusters must lead to structural frustrations in the investigated samples. ij-pair-distances, marked by dashed ellipses, are clearly shorter than the first maximum of $g_{ij}(r)$, here given by corresponding side lengths of the sketched-in elementary triangles (ET). The gray area cannot be filled by *sss* ET. b) Video image of a supercooled binary 2D colloidal mixture. Neighboring big and small particles are connected by a thin line, and two neighboring small colloids, both neighbored to a big one, by a thick line. Thus, structural frustrations for the cases in a) can nicely be seen, except for *bbb*/*bbs* multi crystallite clusters.

sss 3-particle combination are hexagonally packed. The *bbs* CC have a square body-centered lattice, and for *bss* CC ten small colloids around a big one shape a decagonal cell. CC are presented in the upper part of fig. 1b and highlighted in the enlarged pictures of fig. 2. Some MCC are shown in figs. 2b, d and fig. 3a. The existence of ET could already be demonstrated in the same binary 2D sample analyzing 3-point correlation functions [8].

For touching hard discs of big and small colloids the particles are densely packed, as shown in the lower part of fig. 1b. However, small structural mismatches for the HDA will be equally distributed in the real system because of the repulsive particle interaction since those structures locally join better than the triangles of HDA in the monolayer. For example, the 4 big particles of *bbs* CC evenly share the structural mismatch and this is why the *bbs* ET become rectangular. Additionally, for 10 small colloids around one big particle, the MFR of the small colloids have to overlap slightly (compare with fig. 2), which is why such rings of 10 small particles are often seen to be distorted, as shown in fig. 3b. Thus, the ET are local density-optimized with respect to the repulsive interaction. Each of the four different ET occur at the same time (see fig. 2).

Qualitative description of the peaks of $g_{ij}(r)$. – In the past, the origin of the split second maximum of $g_{ij}(r)$ have been intensively investigated in order to understand the amorphous local glass structure. In three-dimensional (3D) simulation of a simple composed Lennard-Jones glass former [9], the split second maximum is related to a distorted face-centered cubic (fcc) packing, since the pair-distances of the radial pair-distribution functions partially correspond with the peak positions of pure fcc structure. In [10] 13-atomic icosahedral clusters are observed, as shown by Voronoi polyhedron analysis coupled with radial pair-distribution functions. In another 3D colloidal suspension the microscopic structure, measured by confocal microscopy and analyzed by the bond order parameter method, is mainly related to fcc and hexagonally close-packed clusters as well as fragments of icosahedra [11]. Also local structural analysis by Voronoi analysis of particle topologies has been reported for simulations of a binary mixture in 2D [12]. In this case, the split second maximum of the partial radial pair-distribution functions $g_{ij}(r)$ were not applied. In this context, interesting tiling studies of single-component 2D liquids should be mentioned, developed to investigate 2D melting by a plane tessellation of squares and triangles [13] or by local defect polygons [14].

Up to now, the microscopic amorphous structure of glass formers is typically investigated by a Voronoi polyhedron analysis or by the bond order parameter, in which the entire nearest neighborhood around each particle is considered simultaneously. In this paper, the local

amorphous particle configurations of a 2D binary colloidal glass former is taken to be triangles of nearest-neighboring particles (TNNP) in 2D, filling up the corresponding monolayer completely. The TNNP shapes are attributed by a limited number of idealized local densely packed structures, termed as elementary triangles (ET). In the following, the peak positions of the partial radial pair-distribution functions will be qualitatively described by pair-distances originating from varying combinations of different ET, forming CC and MCC.

In [4] the authors observed in a comparable binary 2D system, that for increasing Γ the first peak of the partial radial pair-distribution functions, $g_{ij}(r)$, becomes more pronounced and narrower in width, and the first minimum decreases in magnitude while a splitting of the second maximum becomes increasingly visible. Since no long-range order appears, the temperature dependence of $g_{ij}(r)$ is characteristic for glass formers. In this paper, the features of $g_{ij}(r)$ are analyzed solely for strongly supercooled liquids with split second maximum.

The first maximum of each pair ij of $g_{ij}(r)$ refers to side lengths of ET. Common edges between two ET —also of different kind— connect these triangles without any structural mismatch, *i.e.* they are still local density-optimized (compare with fig. 3a). Pair-distances of different two-particle combinations for various CC or MCC are calculated (using the first maximum of $g_{ss}(r)$ for ss sides of sss ET, the first maximum of $g_{bb}(r)$ for bb sides of bbb and bbs ET and the first maximum of $g_{bs}(r)$ for bs sides of bss ET). The resulting vertical lines, sketched in fig. 4, approximately determine the near-zone peaks of $g_{ij}(r)$. Moreover, it appears that the clearly separated big peaks have an additional, but hidden inner structure consisting of different peaks, which belong to various particle configurations.

Random tiling of the four different kinds of ET does not cover the monolayer faultlessly, as shown in fig. 3a. At places, where the tiling fails, structural frustrations of the local particle arrangements arise and the repulsive interaction distorts the shape of the triangles leading to less densely packed TNNP depending on the local particle distribution. Such structural frustrations as well as the thermal particle fluctuations are responsible for broadened first maxima and for the poorer resolution of the peaks of larger pair-distances in $g_{ij}(r)$. The loss of long-range order in $g_{ij}(r)$ follows additionally from the increasing number of possible ET-combinations for increasing pair-distance.

Structural frustration is strong for CC-like TNNP structures of small sizes if the various ET do not fit well among each other. In the investigated binary 2D system, mainly bss TNNP are disturbed by structural frustration because the ten-fold symmetry does not suit to the other kinds of ET (compare with figs. 4a-c).

Notice that pair-distances, calculated by CC or MCC, are not equivalent to mean values of pair-distances for the corresponding perturbed TNNP combinations. These distributions cannot be described by Gaussian or Lorentzian fits. For example, the largest ss distance of two bss ET with a common bs side are densely packed and therefore, the calculated pair-distance should be shorter than those pair-distances of two structural frustrated bss TNNP. Additionally, the pair-distance distribution of those structural frustrated TNNP should be broad. Furthermore, for the largest ss distance of two opposite bss ET with the same b colloid, the calculated pair-distance of CC should be a little bit longer than those pair-distances of two structural frustrated bss TNNP. Their pair-distance distribution should be rather sharp. Thus, the positions of the sketched vertical lines relating the positions of the peaks of the $g_{ij}(r)$ always depend on the special particle configuration itself. By these considerations the calculated pair-distances of CC or MCC lead to the nearest-neighboring peak of $g_{ij}(r)$, as seen in fig. 4. These justify the previous statements that the calculated pair-distances of CC and MCC approximately determine the near-zone peaks of $g_{ij}(r)$.

In fig. 4b the pair-distance bs for the combination of a bbs and a bbb ET, which occurs at $\sim 46\,\mu$m for $g_{bs}(r)$, is rather rare. This is also true for the probability of the pair-distance bb

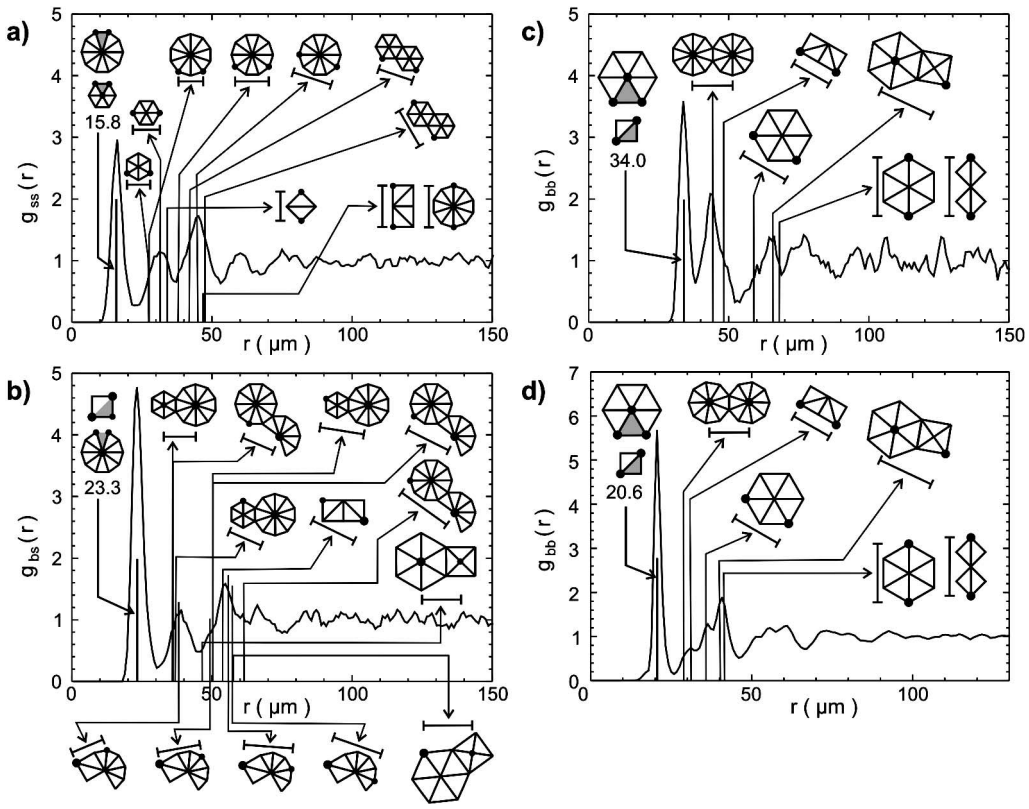

Fig. 4 – a)-c) Partial radial pair-distribution functions $g_{ij}(r)$ for the three possible pairs *ss*, *bs*, and *bb* of the binary 2D colloidal suspension shown in fig. 2 with $\Gamma = 411$, $B = 7.00\,\mathrm{mT}$, and $\xi = 0.70$. d) $g_{bb}(r)$ of a binary 2D colloidal mixture with $\Gamma = 867$, $B = 3.84\,\mathrm{mT}$, and $\xi = 0.356$. In each case, idealized distances of *ss*, *bs* or *bb* pairs for crystallite clusters (CC) or multi crystallite clusters (MCC) of idealized ET are sketched by vertical lines. Thus, the near-zone maxima can approximately be described. Examples for such CC and MCC can be found in fig. 2 and fig. 3b. Notice that not all combinations of elementary triangles (ET) are plotted because of clarity, specially for possible *ss*-pair-distances. However, the simplification does not affect the line of arguments. Different peak intensities of $g_{bb}(r)$ in c) and d) can be explained by their different number ratios ξ. For d), because of different magnetic fields the ratio between the magnetic susceptibilities of big and small colloids is different compared with a)-c). Thus, the MFR ratio of big to small colloids was determined to be 1.89 and the real *bs*-pair-distance is about 2.5% smaller than that calculated by HDA. The *bbs* ET are still rectangular while for *bss* ET only nine small particles fit around a big one.

of the long diagonal for the combination of two *bbb* triangles in fig. 4c, which lies at $\sim 58\,\mu\mathrm{m}$ for $g_{bb}(r)$. These weak signals result because $\xi = 0.70$, so that there are many more small than big colloids (compare with fig. 2). However, in fig. 4d with $\xi = 0.356$, *i.e.* many more big than small colloids, the signals of the split second maximum of $g_{bb}(r)$ mainly belong to combinations between *bbb* ET, while the peak of two *bss* ET with common *ss* side can be mostly neglected. Thus, the amplitudes of near-zone peaks of $g_{ij}(r)$ correspond to ξ.

Conclusions. – In the investigated binary 2D colloidal glass former, a hard-disc approximation (HDA) is deduced from the first maxima of $g_{ij}(r)$. Using simple geometric argu-

ments, the following characteristic features about the amorphous microscopic structure in the monolayer were observed. First, the colloids tend to form local density-optimized particle arrangements, called elementary triangles (ET). Second, there is one ET for each 3-particle configuration. Third, the ET tend to conglomerate. The split second maximum of $g_{ij}(r)$ can be accounted for by different crystallite clusters (CC) and multi crystallite clusters (MCC). Fourth, there are structural frustrations because of packing mismatches of CC and MCC, which is why all maxima of $g_{ij}(r)$ are additionally broadened. Fifth, the peak intensities of $g_{ij}(r)$ depend on the number ratio between big and small particles. Sixth, the large number of possible combinations for the tiling of different ET and structural frustrations lead to the loss of long-range order.

To clarify the general importance of describing amorphous systems by various local density-optimized ET as well as CC and MCC, particle coordinates of other glass formers have to be investigated in the same way. For binary 2D mixtures with different size ratios of big to small particles, other *bbs* and *bss* ET should exist. In 2D systems of more than two components, additional kinds of ET are expected. In 3D, triangles have to be replaced by tetrahedrons [15]. For systems with complicated particle interactions such as covalent bonds or for polydisperse colloidal suspensions, the simple argument of local density-optimized structures must be adapted appropriately.

* * *

The author thanks K. Zahn, G. Maret, R. Haussmann, U. Gasser and J. Horbach for discussions, the SFB 513 of the Deutsche Forschungsgemeinschaft for financial support and the Marie Curie Network No. MRTN-CT-2003-504712.

REFERENCES

[1] Vilgis T. A., *Disordered Effects on Relaxational Processes*, edited by Richert R. and Blumen A. (Springer-Verlag, Berlin) 1994, p. 153.
[2] Ediger M. D., Angell C. A. and Nagel S. R., *J. Chem. Phys.*, **100** (1996) 13200.
[3] Zahn K., Mèndez-Alcaraz J. M. and Maret G., *Phys. Rev. Lett.*, **79** (1997) 175.
[4] König H., Hund R., Zahn K. and Maret G., submitted to *Eur. Phys. J. E.*
[5] König H., Zahn K. and Maret G., *Proceeding of Slow Dynamics in Complex Systems*, edited by Tokuyama M. and Oppenheim I., *AIP Conf. Proc.*, **708** (2004) 40.
[6] König H., *Mikroscopische Prozesse am Glasübergang einer binären paramagnetischen 2D Kolloidsuspension: Lokal-dichteoptimierte Kristallit-Cluster*, Thesis, University of Konstanz (2002).
[7] *DYNAL PARTICLES AS* (`http://www.dynalbiotech.com`).
[8] König H., *Proceeding of Slow Dynamics in Complex Systems*, edited by Tokuyama M. and Oppenheim I., *AIP Conf. Proc.*, **708** (2004) 76.
[9] Abraham F. F., *J. Chem. Phys.*, **72** (1980) 359.
[10] Kondo T., Tsumuraya K. and Watanabe M. S., *J. Chem. Phys.*, **93** (1990) 5182.
[11] Gasser U., Schofield A. and Weitz D. A., *J. Phys. Condens. Matter*, **15** (2003) 375.
[12] Perera D. N. and Harrowell P., *Phys. Rev. E*, **59** (1999) 5721.
[13] Collins R., *Proc. Phys. Soc.*, **83** (1964) 553.
[14] Glaser M. A. and Clark N. A., *Adv. Chem. Phys.*, **83** (1993) 543.
[15] In three dimensions (3D), tetrahedrons of nearest-neighboring particles (TNNP) and elementary tetrahedrons (ET) have to be considered. ET-like TNNP also form crystallite clusters (CC) and multi crystallite clusters (MCC). In 3D structural frustration occurs as well.